

SLUG FLOW CHARACTERISTICS OVER HILLY-TERRAIN USING THE TWO FLUID MODEL

João N. E. Carneiro, carneiro@td.mw.tum.de

Angela Ourivio Nieckele, nieckele@mec.puc-rio.br

Departamento de Engenharia Mecânica – Pontifícia Universidade Católica de Rio de Janeiro, PUC-Rio
R. Marques de São Vicente 225 – Rio de Janeiro, RJ, Brasil

Abstract. *At the present work a numerical analysis of the slug flow in inclined pipelines is performed aiming to improve the understanding of slug flow characteristics over hilly-terrain section. Three types of pipelines are investigated: horizontal, descending and a “V” section pipeline. An air and oil two-phase fluid mixture is examined. The flow field is determined based on the two-fluid model by the solution of the momentum conservation equations for each phase, continuity of the gaseous phase and total mass conservation. Since the pipelines are very long, the flow is considered as one-dimensional. The finite volume method is employed to solve the conservation equations. It is shown that the mean length is approximately the same for the horizontal and descending case, where the gravity effect is negligible due to the high velocities. However, larger slug lengths are observed along the “V” section pipeline, especially at the ascending section due to the accumulation of liquid at the dip. It can be clearly seen that slug length distribution changes across a symmetrical pipeline, since the gravity effect is not symmetrical.*

Keywords: *slug-flows, one-dimensional, inclined pipelines, two fluid model.*

1. INTRODUCTION

Two-phase flow in the slug pattern can be found in several engineering applications, such as flow of hydrocarbons through pipelines, liquid-vapor flow in power-plants, etc. (Dukler and Fabre, 1992). Slug flow is a two-phase flow pattern which is characterized by a sequence of packs of liquid separated by long gas (Taylor) bubbles flowing over a liquid film inside the pipe, and is normally associated with high pressure-drops and a considerable degree of intermittency in the system. In offshore production systems, for example, stabilized gas and liquid flow rates are normally sought to ensure a proper operation of the plant, and separation equipments are often designed for such conditions. In this sense, previous knowledge of the flow patterns expected are of extreme importance, and if slug flow is likely to occur, it is not only important to know its mean behaviour but also the statistical details — such as the maximum slug length expected, which dictates an proper sizing of receiving equipments.

The slug pattern can be formed in horizontal and inclined pipelines from a stratified pattern by basically two mechanisms: the natural growth of hydrodynamic instabilities and by the accumulation of liquid due to irregularities on the pipeline. In the first case, small perturbations in the form of small waves naturally emerge. These waves can grow to larger waves of the size of the pipeline cross-section (Ansari, 1998). The growth mechanism is the classic *Kelvin-Helmholtz* instability (KH) (Lin and Hanratty, 1986; Fan et al., 1993). These waves can continue to grow, capturing the liquid that flows in front of them until the cross section becomes saturated with liquid, thus forming the slugs. At inclined pipelines, the slug can be formed due to the delay and sub-sequent accumulation of liquid at the down points of the pipeline, leading to a cross section completely filled with liquid. The liquid accumulation at valleys of hilly terrain pipelines with sections of different inclinations is also called *terrain slugging* (Taitel and Dukler, 1976 and 1990; Barnea, 1987; Fabre e Liné, 1992, Al-Safran et al., 2005). Wave coalescence was also observed to be an important mechanism acting on slug formation, specially at higher gas flow rates in horizontal pipes (Lin e Hanratty, 1987; Woods et al, 2006). Also in the *V-section* studied by Al-Safran et al. (2005), this initiation mechanism was observed at relatively high gas-flow rates and low liquid flow rates, where smaller waves were unable to block the elbow. The flow in the slug pattern can also be formed by a combination of the mechanisms described above. Small undulations of the terrain can lead to slug formation in addition to the ones formed by the inherent instabilities of the flow. In these cases, the slug formed by one mechanism interacts with those formed by the other, leading to a complex slug pattern.

The intermittence of the flow in the slug pattern causes large instabilities, which propagates through out the pipeline and any other equipment connected to it. This often increases the design problems and it usually leads to a reduction of the efficiency and/or size of a processing plant. Thus, it is important to be able to predict the beginning and subsequent development of the slug pattern, as well, as the prediction of its characteristics such as size and frequency.

Slug front and tail do not necessarily travel at the same velocities. A complex flow dynamics exists in which slugs may grow, collapse and merge with each other, different slugs having also different speeds (Taitel and Barnea, 1990; Issa and Kempf, 2003). In this process, the mean slug length normally increases in the flow direction, because small slugs are unlikely to be stable — due to bubble wake effects — and often degenerate into long waves that are absorbed by faster slugs (Fabre e Liné, 1992). As a consequence of the fact that slug length, velocity and frequency are interrelated quantities, it follows that the slug frequency is likely to diminish towards the pipe ending (Fabre e Liné, 1992; Tronconi, 1990). As pointed out by several authors (Tronconi, 1990, Barnea and Taitel 1993), the spatial

evolution of slugging in the pipe may require at least about 200 – 300 diameters from the inlet region to achieve a developed flow. Since slugs evolve from randomly generated waves at the gas-liquid interface, the flow can also be expected to have a stochastic behaviour. In this sense, one speaks of a statistical steady state condition when the time averaged slug parameters (e.g., close to the pipe end section) do not change. Flow pattern studies (Barnea, 1987) have shown that the pipe inclination can have a very significant effect on the stratified to slug transition, even at very small angles. It was found out that the stabilizing effect of gravity causes transition from downward stratified flow to occur at higher liquid superficial velocities (for a given gas superficial velocity), while for upward sections the transition is anticipated.

When slugs travel through a hilly terrain pipeline with different pipe inclinations, they probably undergo a change in its characteristics when moving from section to section. In addition, slugs can be generated at low elbows (*V-sections*) or dissipated at top elbows (*λ -sections*) originating a very complex pattern (Zheng et al., 1994). Al-Safran et al. (2005) conducted an experimental study of the slug flow characteristics over a hilly terrain pipe with a *V-section*. The analysis was performed focusing on the mechanisms of slug initiation and characteristics of slugs initiated at the lower dip. An attempt was also made in order to group sets of superficial gas and liquid velocities in flow categories (superimposed on typical steady state flow pattern maps for the downhill upstream pipe), according to the influence of the *V-section* on the characteristics of developed slug flow upstream of the downward pipe. Carneiro and Nieckele (2007) analyzed numerically the same problem as Al-Safran et al (2005) and they were able to predict the same trends as observed experimentally.

As described by Issa and Kempf (2003), transient models in the context of pipeline slugging usually solve the Two-Fluid Model equations (Ishii, 1975) in its transient one-dimensional version and can be grouped into three categories: *empirical slug specification*, *slug tracking* and *slug capturing*. In contrast to the other ones, a key feature of the *slug capturing* methodology is the capability of predicting the evolution from stratified to slug flow in a natural manner, i.e., there is no need to incorporate any transition criteria assuming that slugs were generated somehow in the pipe (e.g., by use flow pattern maps). This means that the natural outcome of the solution of the equation system can be either the maintenance of stratified flow in the pipe, or the change in regime if conditions are such that slugs develop in the system. If transition occurs, slugs may grow or decay as they travel downstream in the pipe, and no empirical correlations for slug parameters need to be specified. Thus, the set of equations is maintained even when the regime changes and the slug dynamics is an automatic consequence of the solution of the system.

At the present work, the Two Fluid Model is employed to predict the slug formation in horizontal and slightly inclined pipeline. Good agreement is obtained between the present results and the experimental data of Al-Safran et al. (2005).

2. MATHEMATICAL MODELLING

The mathematical model selected is based on the *slug capturing* technique, in which the slug formation is predicted as a result of a natural and automatic growth of the hydrodynamic instabilities (Issa and Kempf, 2003; Carneiro et al, 2005). Both stratified and slug pattern are modeled by the same set of conservation equations based on the Two-Fluid Model. Additionally, closure relations are also included. The liquid is considered as incompressible, while the gas follows the ideal gas law, $\rho_G = P/(RT)$, where R is the gas constant and T is its temperature, which was considered here as constant. Pressure P was considered constant long the cross section, being the same, for the liquid P_L , gas P_G and interface ($P = P_G = P_L$). Additionally, it was assumed that there is no mass transfer between phases. The governing mass and momentum equations in the conservative form can be written as

$$\frac{\partial(\rho_G \alpha_G)}{\partial t} + \frac{\partial(\rho_G \alpha_G u_G)}{\partial x} = 0 \quad , \quad (1)$$

$$\frac{\partial(\rho_L \alpha_L)}{\partial t} + \frac{\partial(\rho_L \alpha_L u_L)}{\partial x} = 0 \quad , \quad (2)$$

$$\frac{\partial(\rho_G \alpha_G u_G)}{\partial t} + \frac{\partial(\rho_G \alpha_G u_G^2)}{\partial x} = -\alpha_G \frac{\partial P}{\partial x} - \rho_G \alpha_G g \sin(\beta) - \rho_G \alpha_G g \frac{\partial h}{\partial x} \cos(\beta) - F_{Gw} - F_i \quad , \quad (3)$$

$$\frac{\partial(\rho_L \alpha_L u_L)}{\partial t} + \frac{\partial(\rho_L \alpha_L u_L^2)}{\partial x} = -\alpha_L \frac{\partial P}{\partial x} - \rho_L \alpha_L g \sin(\beta) - \rho_L \alpha_L g \frac{\partial h}{\partial x} \cos(\beta) - F_{Lw} + F_i \quad , \quad (4)$$

where $\alpha_G + \alpha_L = 1$. The subscripts G , L , and i concern the gas, liquid phases and interface, respectively. The axial coordinate is x , ρ and α are the density and volumetric fraction, u is the velocity. The pipeline inclination is β , h is the

liquid level inside the pipe, and g is the gravity acceleration. The third term on the right side of Eqs. (3) and (4) are related with the hydrostatic pressure at the gas and liquid, respectively.

The term $F = \tau S / A$ is the friction force per unit volume between each phase and the wall and between the phases (at the interface), where τ is the shear stress, S is the phase perimeter and A is the pipe cross section area. The shear stress is $\tau = f \rho |u_r| u_r / 2$, where u_r is the relative velocity between the liquid and wall, the gas and wall, or gas and liquid. Closure relations are needed to determine the friction factor f , which is a function of the Reynolds number (\mathbf{Re}_G ; \mathbf{Re}_i and \mathbf{Re}_L for the gas, interface and liquid, respectively). defined as

$$\mathbf{Re}_G = \frac{4 A_G u_G \rho_G}{(S_G + S_i) \mu_G}, \quad \mathbf{Re}_i = \frac{4 A_G |u_G - u_L| \rho_G}{(S_G + S_i) \mu_G}, \quad \mathbf{Re}_L = \frac{4 A_L u_L \rho_L}{S_L \mu_L}, \quad \mathbf{Re}_L^s = \frac{\rho_L U_{sL} D}{\mu_L} \quad (5)$$

where μ is the absolute viscosity and D is the pipe diameter. The last Reynolds in Eq. (5) is based on the liquid superficial velocity, i.e., the ratio of the liquid volume flow rate to the total cross section area of the pipe $U_{sL} = Q_L / A = \alpha_L u_L$. The Hagen-Poiseuille formulas were employed for the gas-wall and interface laminar friction factor, corresponding to Reynolds number smaller the 2100, as

$$f_G = \frac{16}{\mathbf{Re}_G}, \quad f_i = \frac{16}{\mathbf{Re}_i}, \quad f_L = \frac{24}{\mathbf{Re}_L^s} \quad (6)$$

For the turbulent regime, the correlation of Spedding & Hand (1991) was employed for the liquid-wall friction factor, while the correlation of Taitel & Dukler (1976) was adopted for the gas-wall and interface friction factor

$$f_G = \frac{0.046}{\mathbf{Re}_G^{0.25}}, \quad f_i = \frac{0.046}{\mathbf{Re}_i^{0.25}}, \quad f_L = \frac{0.0262}{(\alpha_L \mathbf{Re}_L^s)^{0.139}}, \quad (7)$$

The geometric parameters such as gas and liquid areas (A_G, A_L), wetted perimeters (S_G, S_L), and interface width S_i were obtained from the liquid height h (Carneiro et al, 2005).

3. NUMERICAL METHOD

The conservation equations were discretized by the Finite Volume Method (Patankar, 1980). A staggered mesh was employed, with both phases' velocities stores at the control volume faces and all other variables at the central point. Figure 1 illustrates the mesh, where the upper case symbols refer to the main node and lower case symbols to control volume faces. The interpolation scheme *upwind* and the implicit *Euler* scheme were selected to evaluate the space and time derivatives, respectively. The time step was specified to guarantee a Courant number equal to 0.5 (Issa and Kempf, 2003), therefore, the time step was obtained from $\Delta t = 0.5 \Delta x_i |u_{max}|$, where u_{max} is the maximum velocity in the domain. For each time step, due to the non linearities of the problem, the sequence of conservation equations were solved in an iterative process, until convergence was obtained, that is, until the residue of all equations became smaller than 0.0001.

The set of equations (1) though (4) were employed to determined the gas volumetric fraction, the velocities and pressure as described next.

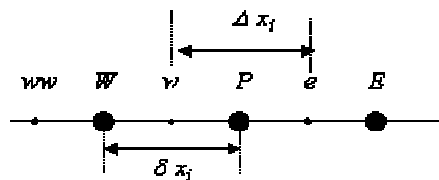


Figure 1. Control volume

3.1. Volumetric fraction

The mass conservation equation for the gaseous phase, Eq. (1) is discretized for the main control volume. The volumetric fraction is obtained from its previous value, α^o , by solving the following discretized equation

$$a_P \alpha_P = a_E \alpha_E + a_W \alpha_W + b \quad (8)$$

$$a_W = \|\tilde{F}_W, 0\| \quad ; \quad a_E = \|\tilde{F}_E, 0\| \quad ; \quad a_P^o = \rho_P^o A \frac{\Delta x_i}{\Delta t} \quad ; \quad a_P = a_W + a_E + a_P^o \quad ; \quad b = a_P^o \alpha_P^o \quad (9)$$

$$\tilde{F}_W = \rho_W u_W A \quad ; \quad \tilde{F}_E = \rho_E u_E A \quad ; \quad \rho_W = (\rho_W + \rho_P)/2 \quad ; \quad \rho_E = (\rho_P + \rho_E)/2 \quad (10)$$

where the symbol $\|a, b\|$ means the maximum between a and b .

3.2. Velocities

Both phases' velocities are obtained from the momentum equation, Eq. (3) and (4), discretized for the staggered control volume. Since pressure is unknown, it is kept explicitly in the equation. Further, due to the non-linearity characteristic of the momentum equation, an under-relaxation factor, γ is also included.

$$a_W u_W = a_{WW} u_{WW} + a_E u_E + b - \alpha_W A (P_P - P_W) \quad (11)$$

$$a_{WW} = \|F_W, 0\| \quad ; \quad a_E = \|-F_P, 0\| \quad ; \quad F_P = (\tilde{\alpha}_W \tilde{F}_W + \tilde{\alpha}_E \tilde{F}_E)/2 \quad ; \quad F_W = (\tilde{\alpha}_{WW} \tilde{F}_{WW} + \tilde{\alpha}_W \tilde{F}_W)/2 \quad (12)$$

$$a_W^o = \rho_W^o \alpha_W^o A \frac{\delta x_i}{\Delta t} \quad ; \quad a_W = (a_{WW} + a_E + a_W^o + S_P \delta x_i)/\gamma \quad ; \quad b = a_W^o u_W^o + S_C \delta x_i + (1 - \gamma) a_W u_W^* \quad (13)$$

where the volumetric fraction at the faces are obtained from their corresponding upwind values, in order to guarantee mass conservation in the staggered control volume. u_W^* corresponds to the velocity of the previous iteration. The source terms S_C e S_P for the gaseous phase are:

$$S_P = \frac{1}{2} f_{G,w} \rho_{g,w} S_{g,w} |u_{g,w}| + b_{int} \quad ; \quad b_{int} = \frac{1}{2} f_{i,w} \rho_{g,w} S_{i,w} |u_g - u_l|_w \quad (14)$$

$$S_C = -\rho_{g,w} \alpha_{g,w} g A \sin(\beta) + -\rho_{g,w} \alpha_{g,w} g A \cos(\beta) \frac{h_P - h_W}{\delta x_i} + b_{int} u_{l,w} \quad (15)$$

In these equations, the volumetric mass fraction is obtained at the faces by linear interpolation, $\alpha_w = (\alpha_W + \alpha_P)/2$. The geometric parameters, S_g and S_i are determined from the volumetric fraction, and the friction factors $f_{G,w}$ and $f_{i,w}$ by Eqs. (6) and (7) applied at the control volume faces. The liquid momentum equation is discretized on a similar manner.

Since the gas momentum equation becomes singular when the gas volumetric fraction becomes zero, this equation must not be solved when a slug is formed ($\alpha_g < 0.02$), and the gas velocity is arbitrarily set to zero, as recommended by Issa e Kempt (2003) and Bonizzi and Issa (2003).

3.3. Pressure

The pressure equation is derived from a combination of both phases' continuity equations, Eqs. (1) and (2), resulting in an overall continuity equation. Since the order of magnitude of the density of each phase is quite different, each equation is normalized by a reference density, resulting in

$$\left[\frac{(\rho_P \alpha_P - \rho_P^o \alpha_P^o)_g}{\rho_{g,ref}} + (\alpha_P - \alpha_P^o)_l \right] \frac{A \Delta x_i}{\Delta t} + \left[\frac{\rho_{e,g} \tilde{\alpha}_{e,g}}{\rho_{g,ref}} u_{e,g} - \frac{\rho_{w,g} \tilde{\alpha}_{w,g}}{\rho_{g,ref}} u_{w,g} \right] A + [\tilde{\alpha}_{e,l} u_{e,l} - \tilde{\alpha}_{w,l} u_{w,l}] A = 0 \quad (16)$$

The pressure is introduced in the global mass conservation equation through its relation with the velocity and density, from both momentum equations and the equation of state for the gas, respectively. The momentum equation, Eq. (11), can be rewritten in an explicit form as:

$$u_W = \hat{u}_W - (\alpha_W A / a_W) (P_P - P_W) \quad \text{where} \quad \hat{u}_W = (a_{WW} u_{WW} + a_E u_E + b) / a_W \quad (17)$$

Substituting Eq. (17) and the ideal gas law in Eq. (16), the discretized equation for the pressure is

$$a_P P_P = a_W P_W + a_E P_E + b \quad ; \quad a_P = a_W + a_E + a_P^o \quad (18)$$

$$a_W = \left(\frac{\rho_{g,w} \tilde{\alpha}_{g,w}}{\rho_{g,ref}} \frac{\alpha_{g,w} A}{a_{w,g}} + \tilde{\alpha}_{l,w} \frac{\alpha_{l,w} A}{a_{w,l}} \right) A ; a_E = \left(\frac{\rho_{g,e} \tilde{\alpha}_{g,e}}{\rho_{g,ref}} \frac{\alpha_{g,e} A}{a_{e,g}} + \tilde{\alpha}_{l,e} \frac{\alpha_{l,e} A}{a_{e,l}} \right) A ; a_P^o = \frac{\alpha_{g,P} A \Delta x_i}{P_{ref} \Delta t} \quad (19)$$

$$b = \left[\left(\frac{\rho_{g,w} \tilde{\alpha}_{g,w}}{\rho_{g,ref}} \hat{u}_{g,w} + \tilde{\alpha}_{l,w} \hat{u}_{l,w} \right) - \left(\frac{\rho_{g,e} \tilde{\alpha}_{g,e}}{\rho_{g,ref}} \hat{u}_{g,e} + \tilde{\alpha}_{l,e} \hat{u}_{l,e} \right) \right] A + a_P^o P_P^o - \frac{(\alpha_P - \alpha_P^o) l A \Delta x_i}{\Delta t} \quad (20)$$

When a slug is formed, the contribution from the gas phase must be eliminated from the overall mass conservation equation.

4. RESULTS

At the present work a numerical analysis of the slug flow in inclined pipelines is performed aiming to improve the understanding of slug flow characteristics over hilly-terrain section. Three types of pipelines are investigated: horizontal, descending and a *V-section* pipeline.

A *V-section* pipeline was defined based on the experimental work of Al Safran et al. (2005). The pipeline consists of descending and ascending sections with length of 21.34 m, and inclination of $\beta = -1.93^\circ$ and $\beta = +1.93^\circ$ in relation to the horizontal direction as illustrated in Fig. 2a. To guarantee a smooth transition between the downward and upward sections, a small horizontal section of 0.3 m joining the two parts was added. The pipeline diameter is equal to $D=0.0508$ m. The total length of the pipelines is equal to $L=42.98$ m. To investigate the effect of small inclinations in the slug flow parameters, the same conditions were tested in a horizontal pipeline, Fig. 2b, and in a pipeline with a downward inclination of $\beta = -1.93^\circ$, Fig. 2c. All pipelines have the same total length L .

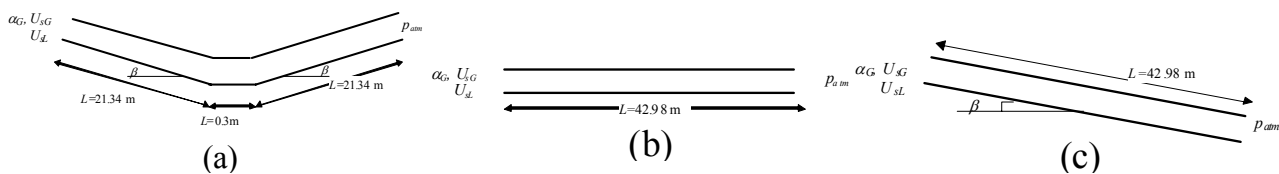


Figure 2. Configurations considered: (a) *V-section* pipeline; (b) horizontal pipeline (c) slightly inclined pipeline

The same two-phase fluid mixture (air and oil) employed by Al-Safran et al. (2005) was defined. The air was considered as ideal gas with gas constant $R=287$ N m/(kg K), with molecular viscosity of $\mu_G=1.796 \times 10^{-5}$ Pa s. The oil density was $\rho_L=890.6$ kg/m³, and molecular viscosity $\mu_L=1.02 \times 10^{-2}$ Pa.s. The inlet liquid holdup α_L was defined as 0.4 ($\alpha_G=0.6$) and a constant atmospheric pressure p_{atm} was kept at outlet.

The initial condition was defined as a stratified steady state flow, that is, constant liquid height along the pipeline, with constant liquid and gas velocities, and pressure distribution obtained by solving the momentum conservation equation, considering equilibrium stratified flow.

Two situations were considered corresponding to gas and liquid superficial velocities defined as $U_{sL} = 0.6$ m/s and $U_{sG} = 0.64$ m/s and $U_{sL} = 1.22$ m/s and $U_{sG} = 1.3$ m/s. Figure 3 illustrates the flow pattern map, built based on the studies of Taitel & Dukler (1976), for the horizontal pipeline ($\beta=0^\circ$) and for the slightly inclined descending pipeline ($\beta = -1.93^\circ$). At these maps the two combinations of superficial velocities are indicated. The square symbol indicates that a slug pattern was obtained and a triangular symbol indicates that a stratified flow was obtained with the present simulations. It can be seen in Fig. 3a for the horizontal case that the slug pattern was obtained for both velocities combinations, confirming the expectation given by the map. For the descending case, the flow pattern map predicts an increase in the stratified flow region; therefore the slug pattern is expected only for one case. This behavior was also predicted by the present simulations.

Based on these results, the two situations considered were classified as Category I and II. The gas and liquid superficial velocities were defined as $U_{sL} = 0.6$ m/s and $U_{sG} = 0.64$ m/s for Category I and $U_{sL} = 1.22$ m/s and $U_{sG} = 1.3$ m/s for Category II.

Figures 4 illustrates successive liquid hold-up profiles along the pipeline in time for Category I cases at the horizontal, descending and *V-section* pipelines, while Fig. 5 corresponds to Category II.

As it can be seen in Fig. 4, for Category I, slug pattern is observed in the horizontal pipeline, Fig. 4a, but it is not observed in the descending pipeline, Fig. 4b, due to the gravity stabilizing effect which inhibits small perturbations to grow at the interface, inducing the slug. For the *V-section* pipeline shown in Fig. 4c, the slug flow is formed by the accumulation of liquid at the dip. This was the same behavior observed experimentally in Al-Safran et al. (2005), for the same superficial velocities.

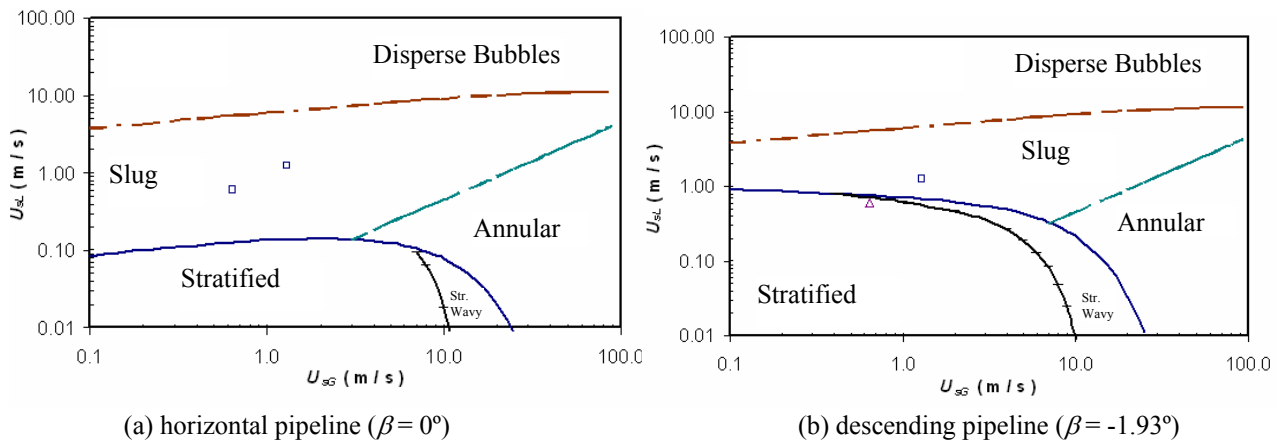


Figure 3. Flow pattern map.

The hold-up profiles in time for Category II, shown in Figs. 5, show that, as opposed to the Category I case, it can be seen that due to same slug formation mechanism, the slugs are formed approximately at 7m from the inlet for all cases. The effect of gravity is to delay just a little the slug formation. It can also be seen, that due to the high frequency, there is not enough time to occur liquid accumulation at the dip of the *V*-section pipeline, therefore, there are no additional slugs being formed. Once again, these observations agree with the experiments of Al-Safran et al. (2005).

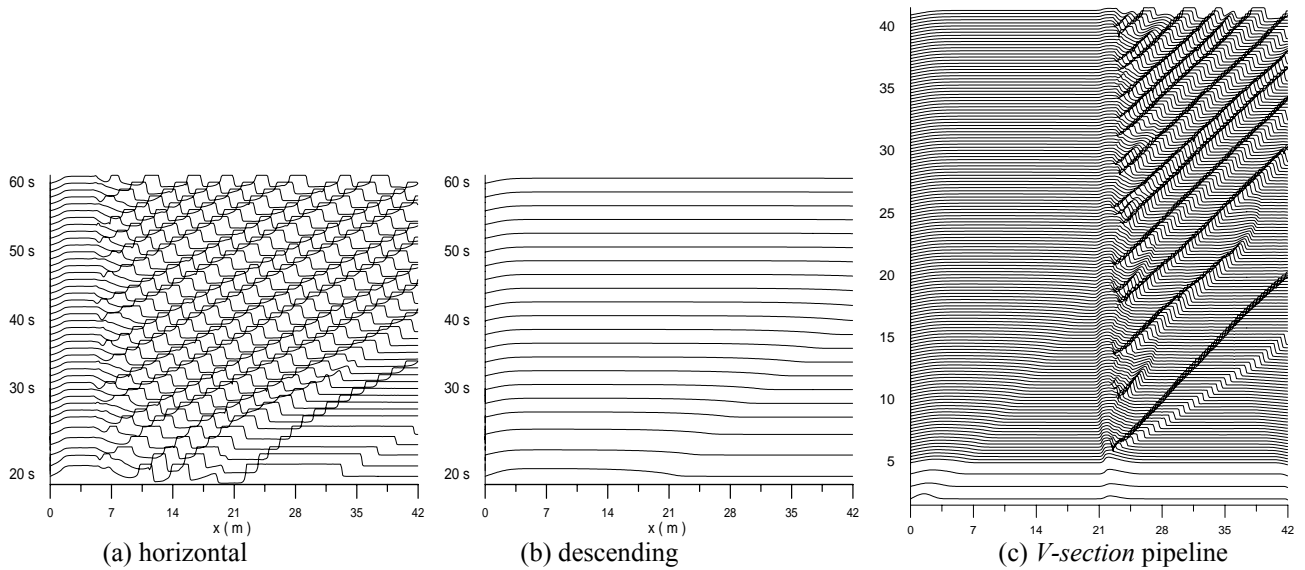


Figure 4. Successive hold-up profiles in time. Category I: $U_{SL} = 0.60$ m/s, $U_{SG} = 0.64$ m/s

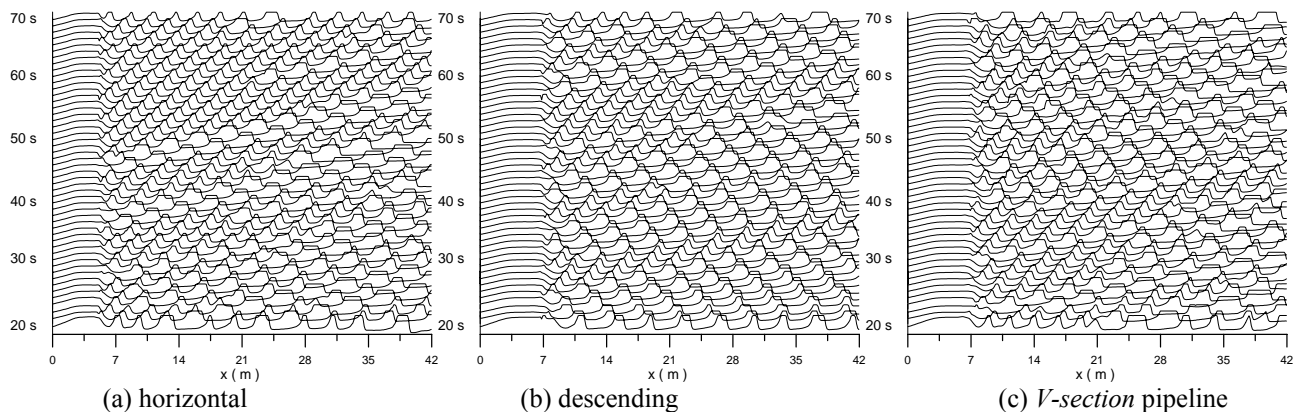


Figure 5. Successive hold-up profiles in time. Category II: $U_{SL} = 1.22$ m/s, $U_{SG} = 1.30$ m/s.

The slug translation velocity U_t , length L_s and frequency ν_s were determined for the three pipelines configurations. The mean slug translation velocity U_t is inferred by the dimensionless parameter C_o , based on the same correlation employed in Issa and Kempf (2003),

$$U_t = C_o U_M + U_d \quad ; \quad \begin{cases} C_o = 1.05 & \text{and} & U_d = 0.54\sqrt{gD}, & \text{if} & Fr_M < 3.5 \\ C_o = 1.20 & \text{and} & U_d = 0, & \text{if} & Fr_M > 3.5 \end{cases} \quad (21)$$

where the mixture velocity U_M is equal to the sum of the inlet liquid and gas superficial velocities, $U_M = U_{sL} + U_{sG}$. The Froude number Fr_M is based on the mixture velocity as $Fr_M = U_M / (gD)^{0.5}$.

The slug parameters corresponding to $x = 37$ m are shown in Table 1. It can be seen that for the first category the liquid accumulation at the dip leads to a superior frequency for the V -section than the horizontal case, since the length is smaller, once the velocities are similar. This tendency was also experimentally observed by Al-Safran et al. (2005). It should be mentioned here, that it was only possible to perform a qualitative comparison, since the data of Al-Safran et al. (2005) were not available due to proprietary restriction.

Table 1. Slugs' characteristics

Category	C_o		ν_s (1 / s)		L_s/D	
	I	II	I	II	I	II
Horizontal	1.25	1.40	0.33	0.95	42.6	13.9
Descending	-	1.39	-	0.94	-	13.5
V -section	1.23	1.37	0.38	0.83	29.6	21.3

Table 1 shows that a slightly higher velocity is found for Category II. The slug length of the horizontal and descending cases differed by 5%, and the frequency was approximately constant. However for the V -section the slug length was 58% larger, leading to a 14% reduction of the frequency in relation to other two cases. The increase in the length is due to the accumulation of liquid at the dip, which did not induce the formation of new slugs, but increased its length. Further the liquid velocity at the ascending section is smaller, what also contributed to increase the slug length.

Figure 6 shows the average slug length along the pipelines for Category II. It can be seen that mean length is approximately the same for the horizontal and descending case, where the gravity effect is negligible due to the high velocities. Larger slug lengths are observed along the V -section pipeline, especially at the ascending section due to the accumulation of liquid at the dip as described previously. It can be clearly seen that slug length distribution changes across a symmetrical pipeline, since the gravity effect is not symmetrical.

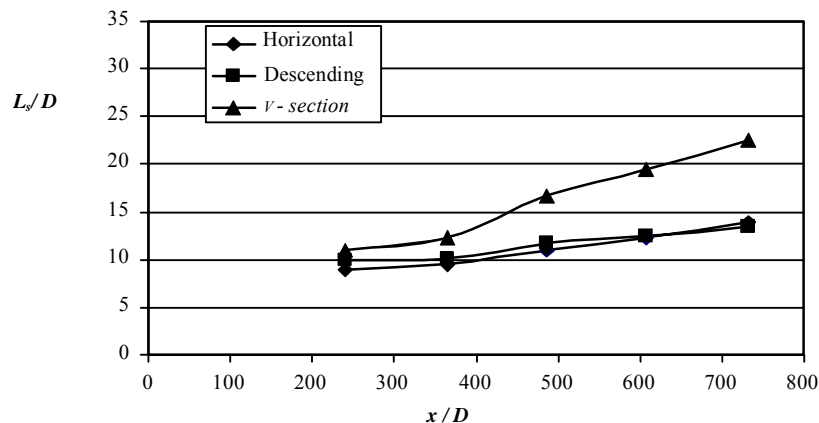


Figure 6. Average slug length along horizontal, descending and V -section pipelines: $U_{sL} = 1.22$ m/s and $U_{sG} = 1.3$ m/s.

5. FINAL REMARKS

The Two Fluid Model was employed to predict the slug formation along horizontal, slightly inclined and V -section pipelines. The results obtained qualitatively agreed with the experimental data of Al-Safran et al. (2005). The flow can be classified in different Categories, depending in the gravity influence to damp the slug formation. The accumulation of liquid in lower sections of the pipeline can increase not only the size of the slug, but also its velocity.

6. ACKNOWLEDGEMENTS

The authors thank the Brazilian Research Council, CNPq for the support awarded to this work.

7. REFERENCES

- Ansari, M. R., 1998, "Dynamical Behaviour of Slug Initiation Generated by Short Waves in Two-phase Air-water Stratified Flow", ASME Heat Transfer Division, Vol. 361, pp. 289-295.
- Al-Safran, E., Sarica, C., Zhang, H.Q. & Brill, J., 2005, "Investigation of Slug Flow Characteristics in the Valley of a Hilly Terrain Pipeline", International Journal of Multiphase Flow, Vol. 31, pp. 337-357.
- Barnea, D., 1987, "A Unified Model for Predicting Flow-Pattern Transitions for the Whole Range of Pipe Inclinations", International Journal of Multiphase Flow, Vol. 13, pp. 1-12.
- Barnea, D. & Taitel, Y., 1993, "A Model for Slug Length Distribution in Gas-Liquid Slug Flow", International Journal of Multiphase Flow, Vol. 19, pp. 829-838.
- Barnea, D. & Y. Taitel, Y., 1994, "Interfacial and Structural Stability of Separated Flow", International Journal of Multiphase Flow, Vol. 19, pp. 387-414.
- Bonizzi, M.; Issa, R.I., 2003, "On The Simulation of Three-Phase Slug Flow in Nearly Horizontal Pipes Using the Multi-Fluid Model", International Journal of Multiphase Flow, Vol. 29, pp. 1719-1747.
- Carneiro, J. N. E. , Ortega, A. J., Nieckele, A. O., 2005, "Influence of the Interfacial Pressure Jump Condition on the Simulation of Horizontal Two-Phase Slug Flows Using the Two-Fluid Model", Proceedings of 3rd International Conference on Computational Methods in Multiphase Flow 2005, Portland, Maine, USA.
- Carneiro, J. N. E. and Nieckele, A. O., 2007, "Investigation of Slug Flow Characteristics in Inclined Pipelines, ", Proceedings of 4th International Conference on Computational Methods in Multiphase Flow 2005, Bologna, Italy.
- Dukler, A.E.; Fabre, J., 1992, "Gas-liquid Slug Flow-knots and Loose Ends", Proceedings of 3rd International Workshop Two-Phase Flow Fundamentals, Imperial College.
- Fabre, J. & Liné, A., 1992, "Modeling of Two-Phase Slug Flow", Annual Review of Fluid Mechanics, Vol. 24, pp. 21-46.
- Fan, Z.; Lusseyran, F.; Hanratty, T.J., 1993, "Initiation of Slugs in Horizontal Gas-liquid Flows", AIChE Journal, Vol. 39, pp. 1741-175.
- Hand, N.P. 1991, "Gas-Liquid Co-Current Flow In A Horizontal Pipe", Ph.D. Thesis, Queen`s University Belfast.
- Ishii, M., 1975, Thermo-Fluid Dynamic Theory of Two-Phase Flow, Eyrolles, Paris.
- Issa, R. I. & Kempf, M. H. W., 2003, "Simulation of Slug Flow in Horizontal and Nearly Horizontal Pipes With the Two Fluid Model", International Journal of Multiphase Flow, Vol. 29, pp. 69-95.
- Lin, Y.P. & Hanratty, T. J., 1987, "Prediction of the Initiation of Slugs With the Linear Stability Theory", International Journal of Multiphase Flow, Vol. 12, pp. 79-98.
- Patankar, S.V., 1980, Numerical Heat Transfer and Fluid Flow, Hemisphere Publishing Corporation.
- Spedding, P.L.; Hand, N.P., 1997, "Prediction in Stratified Gas-Liquid Co-Current Flow in Horizontal Pipelines, International Journal Heat Mass Transfer, Vol. 40, pp. 1923-1935.
- Taitel, Y. & Dukler, A.E., 1976, "A Model for Predicting Flow Regime Transitions in Horizontal and Near Horizontal Pipes", AIChE Journal, Vol. 22, pp. 47-55.
- Taitel, Y. & Barnea, D., 1990, "Two-phase Slug Flow", Advances in Heat Transfer, Vol. 20, pp. 83-132.
- Tronconi, E., 1990, "Prediction of Slug Frequency in Horizontal Two-Phase Slug Flow, AIChE Journal, Vol. 36, pp. 701-709.
- Woods, B. D., Fan, Z. & Hanratty, T. J., 2006, "Frequency And Development of Slugs in a Horizontal Pipe at Large Liquid Flows", International Journal of Multiphase Flow, Vol. 32, pp. 902-925.
- Zheng, G., Brill, J. P. & Taitel, Y., 1994, "Slug Flow Behavior in a Hilly Terrain Pipeline", International Journal of Multiphase Flow, Vol. 20, pp. 63-79.

8. RESPONSIBILITY NOTICE

The authors are the only responsible for the printed material included in this paper.